J. Fluid Mech. (2021), *vol*. 908, A21. © The Author(s), 2020.
Published by Cambridge University Press
doi:10.1017/jfm.2020.862

Slow spectral transfer and energy cascades in isotropic turbulence

Sualeh Khurshid[1], **Diego A. Donzis**[1,†] **and Katepalli R. Sreenivasan**[1,2]

[1]Department of Aerospace Engineering, Texas A&M University, College Station, TX, USA

[2]Department of Mechanical and Aerospace Engineering, Department of Physics and Courant Institute of Mathematical Sciences, New York University, New York, NY, USA

(Received 29 May 2020; revised 17 August 2020; accepted 16 September 2020)

A database of highly resolved direct numerical simulations of three-dimensional isotropic turbulence, with Taylor microscale Reynolds numbers ranging from $\approx$3 to 400, and grid sizes up to 2048^3, is used to analyse the temporal behaviours of spectral transfer and energy that result from low-wavenumber forcing. The temporal behaviours of the energy and energy transfer spectra are analysed using single-time and time-delay statistics. Results show that the energy transfer across a given wavenumber in the inertial range fluctuates by an order of magnitude around its temporal average, and only slow fluctuations have the property of being unidirectional, consistent with classical cascade concepts. All small scales, roughly beyond $k\eta > 0.3$, respond essentially instantly to changes at the large scale.

Key words: isotropic turbulence, turbulence simulation

1. Introduction

The spectral transfer of kinetic energy in wavenumber space is an established subject in the theory of turbulence (e.g. Batchelor 1953; Monin & Yaglom 1975; Domaradzki & Rogallo 1990; Frisch 1995; George & Wang 2004; McComb 2014; Sagaut & Cambon 2018). A key feature of this theory is that the transfer of energy, on the average, is from low wavenumbers (or large scales) to high wavenumbers (or small scales). The spectral locality or otherwise of this unidirectional transfer has been widely studied using the quantity $T(k\,|\,p, q)$, which is the energy transfer to scale k from its nonlinear interactions with wavenumbers p and q (Domaradzki 1988; Domaradzki & Rogallo 1990; Yeung & Brasseur 1991; Ohkitani & Kida 1992; Domaradzki & Carati 2007; Kholmyansky & Tsinober 2008; Domaradzki, Teaca & Carati 2009). A broad conclusion of these studies is that the interactions can be highly non-local but the integrated effect yields a cascade-like local energy transfer between scales of similar size. However, the low Reynolds number in those studies, due to limitations of computing power at that time, did not allow previous researchers to distinguish the inertial range (IR) from the bottleneck region (BR) (Falkovich 1994; Verma & Donzis 2007; Mininni, Alexakis & Pouquet 2008; Donzis & Sreenivasan 2010; Küchler, Bewley & Bodenschatz 2019). They were also unable to consider the different subranges of the dissipative wavenumbers

† Email address for correspondence: donzis@tamu.edu

(Khurshid, Donzis & Sreenivasan 2018). Here, we use well-resolved direct numerical simulations over a range of Reynolds numbers, and use single-time and time-delay statistics to assess the response of small scales to the forcing at large scales, as well as energy transfer across different scale ranges.

Two types of averages are considered in this work. The first is a spatial average over the entire domain, indicated by $\langle \cdots \rangle$, which fluctuates with time. The second is a temporal average over these fluctuations, which are denoted by overbars. We are mostly concerned with temporal fluctuations of space averages, unless otherwise mentioned. Further, in the following, it is convenient to consider different subranges of the dissipative wavenumbers: the bottleneck region (BR) is centred around $0.13k\eta$ – where k is the wavenumber magnitude and η is the Kolmogorov scale $\eta = (\nu^3/\langle\epsilon\rangle)^{1/4}$, ν being the viscosity and $\langle\epsilon\rangle$ being the average energy dissipation rate; the so-called near dissipation region (NDR) is centred around $k\eta$ of 1; and the far dissipation region (FDR) is defined, for specificity, as $k\eta \gtrsim 3$. After providing a few details of simulations in § 2, we present the key results in §§ 3 and 4, and follow up with a brief discussion and summary of conclusions in § 5.

2. Comments on the database

The direct numerical simulation data are acquired from standard pseudo-spectral methods. The Taylor microscale Reynolds number ranges from $R_\lambda \sim 3$ to about 400. The resolution is at least $k_{max}\eta \approx 3$ ($k_{max} = \sqrt{2}N/3$ is the highest wavenumber resolvable by the numerical scheme on a N^3 grid). This resolution is two to three times better than that commonly deemed as adequate for high-R_λ simulations; for the best resolved case, the resolution is as high as $k_{max}\eta \approx 35$. Time stepping is done via a second-order Runge–Kutta method with a constant step size chosen such that the Courant–Friedrichs–Lewy number for the database is kept near 0.3 to accurately resolve extreme events (Yeung, Sreenivasan & Pope 2018). The flow is maintained stationary by forcing in the sphere $|\boldsymbol{k}| \leq 2$, where $\boldsymbol{k}$ is the wavenumber vector. The stochastic forcing (SF) scheme is based on Eswaran & Pope (1988) and has been used extensively in past studies. The deterministic forcing (DF) scheme, based on Donzis & Yeung (2010), maintains constant energy in the same low wavenumbers.

To remove dependencies on initial conditions, we have run the simulations for at least 8 eddy turnover times before statistics are collected. The duration of the simulations over which these statistics are computed is at least 15 eddy turnover times, which was found to be sufficient for statistical convergence. Simulation details are summarized in table 1.

3. Single-time statistics

We recall that the three-dimensional energy spectrum $E(k, t)$ evolves according to

$$\frac{\partial E(k,t)}{\partial t} = T(k,t) - 2\nu k^2 E(k,t) + F(k,t), \tag{3.1}$$

where $T(k, t)$ is the inter-component and inter-scale energy transfer and $F(k, t)$ is the forcing applied at the low wavenumbers (§ 2). Our goal is to study the nature of $E(k, t)$ and $T(k, t)$ in different regions of the k-space, for the two forcing schemes of § 2. The fluctuations outside the forcing sphere ($k > k_f$), in both E and T, are comparable for the SF and DF cases at the same R_λ, even though the energy fluctuations within the forcing sphere ($k \leq k_f$) are exactly zero for DF, suggesting that the fluctuations are the result of

Stochastic forcing (SF)				Deterministic forcing (DF)			
R_λ	N	$k_{max}\eta$	T_s/T_E	R_λ	N	$k_{max}\eta$	T_s/T_E
3	128	30.1	15	3	64	15.7	13
7	128	17.4	23	7	128	17.6	19
10	256	27.8	21	10	256	28.3	10
20	512	34.6	21	15	256	20.5	25
50	1024	24.4	34	47	1024	24.1	18
90	2048	21.1	15	—	—	—	—
140	1024	5.6	33	—	—	—	—
230	1024	2.8	25	—	—	—	—
390	2048	2.8	15	—	—	—	—

TABLE 1. Direct numerical simulation database: the Taylor microscale Reynolds number is defined as $R_\lambda \equiv u_{rms}\lambda/\nu$, where $u_{rms} = (3/2)\overline{\langle u^2(\boldsymbol{x}, t)\rangle}$ (brackets and an overline correspond to space and temporal averages, respectively), and the Taylor microscale λ is defined using this velocity scale along with its time- and space-average gradient; N^3 is the grid resolution; T_s is the duration of the stationary state normalized by the eddy turnover time $T_E \equiv L/u_{rms}$ (L being the longitudinal integral length scale).

nonlinear dynamics of turbulence. Hence, for brevity, all the results presented here are for the SF forcing case.

We write the time average of $E(k, t)$ at a wavenumber k as $E(k) \equiv \bar{E}(k, t) \equiv (1/T_s)\int_0^{T_s} E(k, t)\,\mathrm{d}t$ and T_s is the duration of averaging, as listed in table 1. Similar expressions hold for $T(k)$. Typical time series in energy ($E'(k, t) \equiv E(k, t) - E(k)$) and energy transfer ($T'(k, t) \equiv T(k, t) - T(k)$) are shown in figure 1, normalized by their respective averages. Energy transfer T' is an order of magnitude larger than the average, leading us to the first observation that the statistical mechanics of energy transfer is not unidirectional with minor fluctuations in time, but that of a system that fluctuates wildly around a much smaller time average. The energy itself varies considerably more mildly in the IR and the BR (an order of magnitude smaller than the average); we will attempt to explain this towards the end of § 4. As one approaches the NDR, fluctuations in energy transfer are highly correlated at all wavenumbers (figure 1*c*). Energy fluctuations in the NDR (figure 1*d*) are small and slow.

Finally, in the FDR (figure 1*e*,*f*), we see highly intermittent variations in T', much stronger (relative to their averages) than those at lower wavenumbers, as also reported by Khurshid *et al.* (2018). The variations are similar in E'. Since the energy content in the dissipation range decays rapidly with increasing k, the energy and local transfer are very small and the signal is dominated by large intermittent fluctuations observed in figure 1(*e*,*f*). This behaviour was characterized in Khurshid *et al.* (2018).

We now show in figure 2 the standard deviation ($\sigma(X) \equiv \sqrt{\overline{X'(k, t)^2}}$ with $X = E$ or T) in different wavenumber regions. In the IR, the fluctuations in E (figure 2*a*) are substantially smaller than those in T (figure 2*b*). All fluctuations become weaker as k increases, reaching a minimum at $k\eta \sim 0.13$ for E, and, much more unambiguously, at $k\eta \sim 0.3$ for T, corresponding to the respective bottleneck peaks in their spectra (Falkovich 1994; Verma & Donzis 2007; Donzis & Sreenivasan 2010; Ishihara *et al.* 2016; Küchler *et al.* 2019). Fluctuations in T within the IR decay approximately as $k^{-5/3}$ for $R_\lambda \gtrsim 90$. The minimum

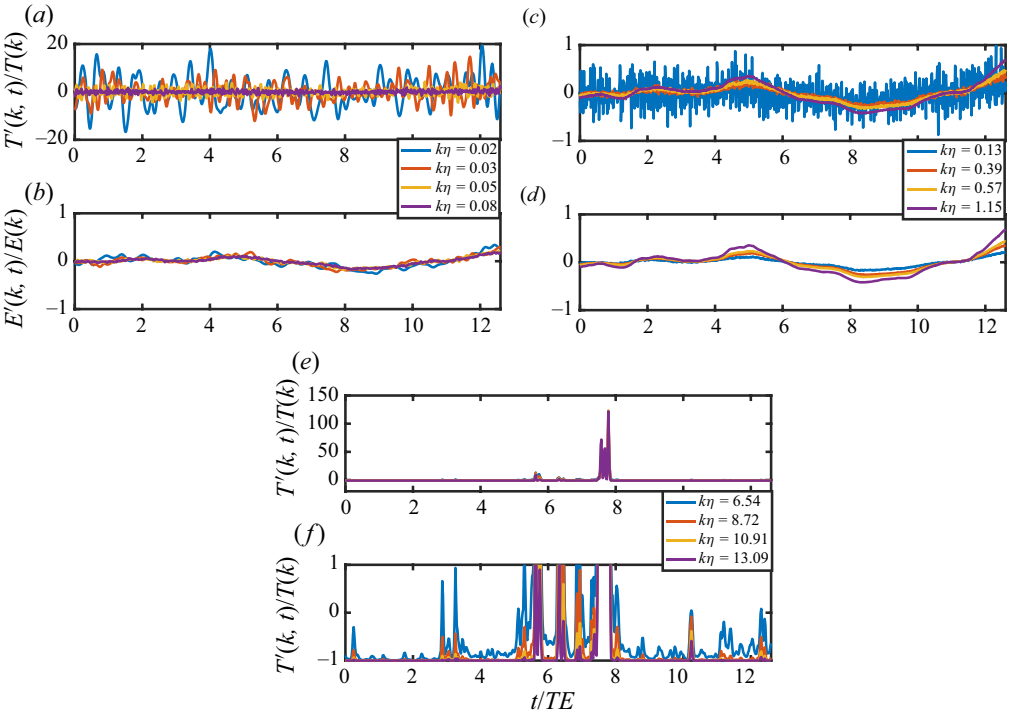

FIGURE 1. Time series of fluctuations in energy and energy transfer in the stationary state; (*a–d*) $R_\lambda \approx 390$. (*a*) Temporal change of the energy transfer at wavenumbers in the IR marked in the legend. The time average of the energy transfer has been subtracted, so the quantity presented is the deviation (or the fluctuation) from the average value, divided by the average. Note that the fluctuations are an order of magnitude larger than the average for the transfer. (*b*) Time series of energy at those same wavenumbers; the fluctuation is of the order of the average. The oscillatory blue line in (*c*) is the energy transfer in the BR, while the others approach the NDR; (*d*) time series for the energy. (*e*) Reynolds number $R_\lambda \approx 90$ and the data are in the FDR; (*f*) the behaviour close to the mean in (*e*). See text for more details.

in the variance of E in the BR is consistent with Ishihara *et al.* (2016), who used a different forcing mechanism from those used here; this suggests that this minimum occurs independent of forcing. The fluctuations in E were recently studied in the context of non-equilibrium corrections to the spectra by Bos & Rubinstein (2017), who proposed that the ratio of non-equilibrium and equilibrium parts of the energy spectra scales as $k^{-2/3}$ in the IR. This scaling was also proposed by Yoshizawa (1994). Using slightly different arguments, Horiuti & Tamaki (2013) showed that this scaling is consistent with the transfer fluctuations decaying as $k^{-5/3}$ in the IR. This scaling of transfer fluctuations is consistent with the direct numerical simulation data in figure 2(*b*). Energy fluctuations, on the other hand, show a weaker decay (approximately $k^{-1/3}$) than predicted by the work cited above. This apparent discrepancy is discussed later in this section.

For wavenumbers beyond the BR, the relative fluctuations grow almost exponentially with the wavenumber in both the energy and transfer spectra. The presence of large and similar-level fluctuations in T to either side of the BR is consistent with our understanding of the BR (Falkovich 1994; Donzis & Sreenivasan 2010). It is also consistent with conclusions from Brasseur (1991) and Brasseur & Wei (1994) where the presence of

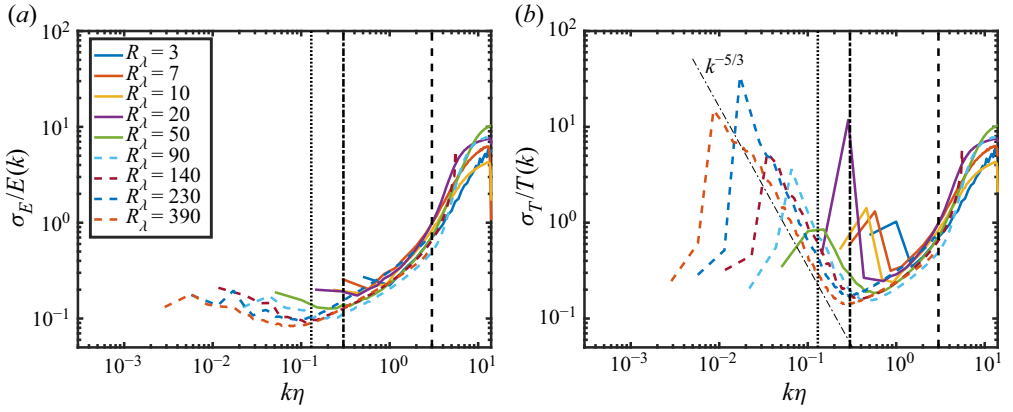

FIGURE 2. Normalized standard deviations $\sigma_E/E(k)$ (*a*) and $\sigma_T/T(k)$ (*b*). The vertical lines correspond to bottleneck peak in the energy spectrum (dotted, $k\eta = 0.13$) and in the transfer spectrum (dashed-dotted, $k\eta = 0.3$), and the boundary between the NDR and FDR (dashed, $k\eta = 3$).

significant non-local interactions between large and dissipative scales was observed; it is similarly consistent with Domaradzki (1988), Domaradzki & Rogallo (1990) and Domaradzki & Carati (2007), where it was shown that non-local interactions in T exhibited strong cancellations when averaged over all pertinent triads, weakening their overall effect in the IR.

We do not observe any statistically significant trends with respect to R_λ for fluctuations in the dissipation range but a slight weakening occurs in the IR.

The main conclusion so far is that the fluctuations of energy transfer T in the IR are large and fast, but those of the energy E are moderate and slow. The fluctuations tend to be of the order of the average as one moves through the BR and then grow again in the NDR becoming large and fast in the FDR.

To pursue this point further, it is useful to separate the slow and fast frequencies demarcated by a frequency ω_c as

$$\frac{E'(k,t)}{E(k)} = E'_<(k,t) + E'_>(k,t), \qquad \frac{T'(k,t)}{T(k)} = T'_<(k,t) + T'_>(k,t), \tag{3.2a,b}$$

where $E'_<(t)$ corresponds to the signal for $\omega < \omega_c$ and $E'_>(t)$ to that for $\omega > \omega_c$, and transfer signals follow the same convention. To be specific, we choose ω_c by decomposing the volume-averaged dissipation, $\langle\epsilon(t)\rangle$, into two parts such that the correlation between $\langle\epsilon(t)\rangle$ and its slow part is higher than 99 %. This is readily done by Fourier-transforming the signals in time and adjusting the filter cutoff ω_c. The decomposition into temporal frequencies is performed on variables ($E'(k,t)$, $T'(k,t)$ and $\langle\epsilon(t)\rangle$) computed from the full velocity field. A physical interpretation of slow and fast modes in terms of classical small and large scales is non-trivial and must invoke the concept of (random) sweeping (Kraichnan 1977).

In figure 3(*a*) we plot the slow part of fluctuations in energy transfer for $R_\lambda \sim 390$. A comparison with figure 1 shows that slow fluctuations are an order of magnitude smaller in the IR than the full signal, as emphasized by their standard deviations (solid line for the slow part and dashed line for the full signal in figure 3*b*). We reach the tentative conclusion here (and consolidate in the next section) that the notion of unidirectional energy transfer

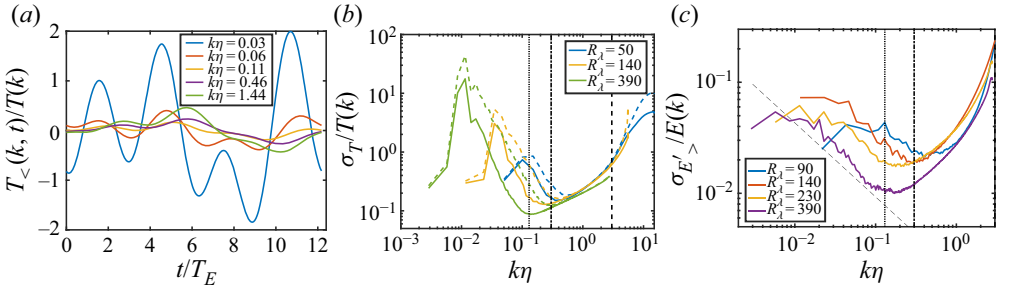

FIGURE 3. (*a*) Time series of slow component of transfer signals for $R_\lambda \approx 390$. The amplitude of the slow component is much smaller than those observed for the full signal in figure 1. (*b*) Normalized standard deviation of slow components (solid line) compared with full transfer signal (dashed line). Slow fluctuations in the IR are weaker in comparison to the full signal, while the two are comparable in the dissipation range. (*c*) The standard deviation of fast fluctuations of energy normalized by the mean energy in the respective wavenumbers. The dashed line corresponds to $k^{-2/3}$. Vertical lines are the same as in figure 2.

in the IR is valid only for slow fluctuations, and is generally not true for the entirety of the energy transfer. In the dissipation range, the slow part of the energy transfer is comparable to that for the full signal. Although no significant changes are observed in slow energy fluctuations, we do observe an approximate $k^{-2/3}$ decay for the fast fluctuations of energy in the IR consistent with predictions of Bos & Rubinstein (2017), as shown in figure 3(*c*). The scaling of fast fluctuations, in both energy and transfer, is thus consistent with the corrections proposed by the non-equilibrium theory.

A more complete description of the statistical behaviour of $E'(k,t)$ and $T'(k,t)$ requires higher-order statistics, on which we will not dwell in any detail here. It suffices to say that the skewness is close to zero in the IR and NDR but increases rapidly in the FDR for both $E'(k,t)$ and $T'(k,t)$, qualitatively similar to the standard deviation in figure 2. A large positive skewness for both T' and E' in the FDR suggests that it is largely sustained by very large (relative) transfers of energy from elsewhere. Such large transfers can only be the result of non-local interactions with energetic wavenumbers. The skewness values of E' and T' in the NDR are comparable to those in the IR.

4. Time-delay statistics

We study the relationships between fluctuations in two wavenumber ranges using a time delay between them. The time-delay correlations for energy will be denoted by $\rho(E'(k_1,t), E'(k_2,t+\tau))$ and those for transfer fluctuations by $\rho(T'(k_1,t), T'(k_2,t+\tau))$. Obviously, if a peak in the correlation $(\rho(X(t)', Y(t+\tau)'))$ occurs at some $\tau < 0$, it implies that the changes in $X(t)$ are correlated with changes in $Y(t)$ after that time lag τ. Each of the quantities is normalized by its standard deviation so that the correlation coefficient ρ ranges between -1 and 1.

Contours of the correlation coefficient for energy and transfer fluctuations between a selected wavenumber ($k_1\eta \approx 0.02$) in the IR and another wavenumber (k_2) with varying time lags (τ) are shown in figure 4, for the highest R_λ. Consistent with observations in figure 1, fluctuations in energy of k_1 for the full signal are well correlated with those at all wavenumbers in figure 4(*a*), and are so with no discernible time lag; this strong correlation is present even in the BR and NDR. This feature suggests that the energy

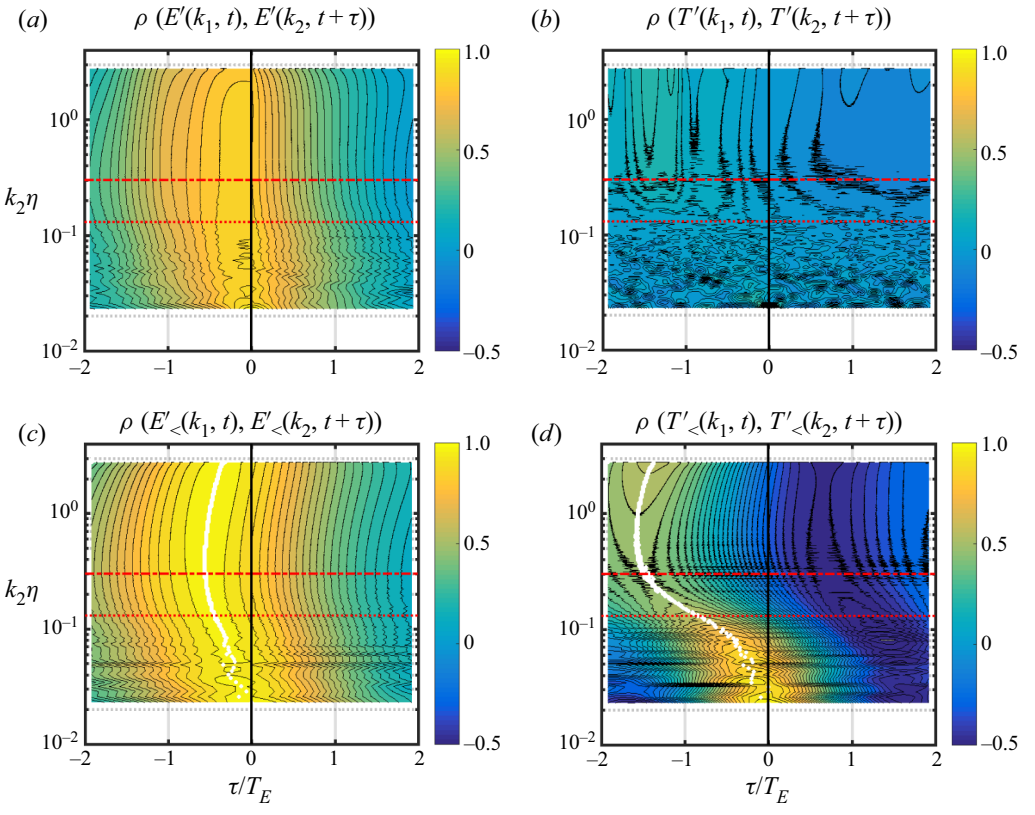

FIGURE 4. Contours of correlations at different time lags τ for E and T at a typical low wavenumber ($k_1\eta \approx 0.02$) with fluctuations at other wavenumbers k_2 for $R_\lambda \sim 390$. Shown are correlations for (*a*,*b*) the full signals and (*c*,*d*) those for their slow components. The horizontal lines are the same as the vertical lines in figure 2. The vertical solid line marks zero lag. The contour levels range from -0.6 to 1 with a constant difference of 0.04.

across wavenumbers is synchronized. We do not observe in figure 4(*a*) any significant improvement in correlations with increasing time lag in the IR.

One possible explanation for the observed synchronicity is the following. The fluctuations of the kinetic energy around their mean value are related to higher-order spectra, associated with fourth-order correlations, etc. Such quantities have been investigated multiple times in the past (Van Atta & Wyngaard 1975; Nelkin & Tabor 1990; Praskovsky *et al.* 1993). The relevant observation for us is that $E_{uu}(k)$, the spectrum of fluctuations of the kinetic energy around their mean value, also scales as $E_{uu}(k) \sim u_{rms}^2 E(k)$. This corresponds to a sweeping-dominated scaling (Kraichnan 1977). Such sweeping implies that the typical temporal behaviour of the spectrum will follow the fluctuations of the velocity, a point we explore in the last section.

This result is contrary to the expectation based on the traditional cascade scenario in which the best correlation would occur with a finite time lag that increases with the wavenumber. On the other hand, the contours shown in figure 4(*c*) suggest that slower wavenumbers are better correlated with increasing time separation, τ. The maximum correlation is indicated using white dots. Slow fluctuations in E at one value of k in the

IR are best correlated with slow fluctuations in another value of k in E when the lag time τ increases; this suggests, for slow fluctuations, a picture that is consistent with the Kolmogorov–Richardson cascade with finite speed.

This synchronous feature is even stronger for energy transfer, shown in figure 4(*b*,*d*), with an interesting behaviour of the peak correlation as one moves to smaller scales. In the IR, the peak correlation of transfer fluctuations with those at large scales is significantly enhanced compared to the full signal. Further, the peak correlation is observed at later times for higher k_2. In the BR, the peak correlation is weaker but the increase in lag is more marked than in the IR, up to $k_2\eta \approx 0.3$, beyond which the peak occurs at a constant lag time of about 1.5 eddy turnover times. This suggests that the slow modes adhere most to a cascade scenario in the IR followed by a seemingly synchronized response of the dissipative ranges. One may speculate that fast fluctuations may well be the result of incomplete cancellation of averages over individual triads in wavenumber shells and correspond to instantaneous transfer. This may be important in models that attempt to capture temporal dynamics assuming only a local scale-by-scale transfer. In the NDR, the peak correlation is independent of the scale.

To address the R_λ trend of the features observed above, we plot the maximum correlation (ρ_{max}) for the full signals and the slow-frequency components of T in figure 5(*a*,*b*) for three R_λ and a fixed $k_1\eta$. Figure 5(*a*) shows correlations from full signals and figure 5(*b*) from slow fluctuations only. We show the correlations between fluctuations at all $k_2 \geq k_1$ for two different k_1, one in the IR (dashed lines) and another in the BR (solid lines). In these figures, a high correlation between disparate wavenumbers does not necessarily mean a non-local interaction as the peak correlation may occur with a lag.

It is immediately evident that stronger correlations occur at higher R_λ for a given pair of k_1 and k_2, but the figures reveal other features worth discussing. For the full signal, figure 5(*a*) shows that the fluctuations in T at all k_2 are largely uncorrelated with fluctuations when k_1 is in the IR. In fact, the correlation drops steeply from a ρ_{max} of 1 when $k_1 \neq k_2$. For k_1 in the BR, stronger correlations are observed at all k_2. For $k_2\eta > 0.3$, the peak correlation is independent of the wavenumber. Together with earlier observations, the fact that the peak correlation time in this range is also independent of k_2 shows that fluctuations in these scales are synchronized across wavenumbers.

The corresponding correlations for slow transfer fluctuations are shown in figure 5(*b*). These correspond to white dots in figure 4 and they confirm the R_λ trend seen in figure 5(*a*). A comparison of figures 5(*a*) and 5(*b*) shows that slow fluctuations are correlated much more strongly than the full signals. The effect of fast fluctuations is thus to reduce the correlation between signals. This reduction effect is stronger at lower R_λ.

For k_1 in the IR, the reduction in correlation with k_2 ($k_2 \neq k_1$) is weaker for the slow part than for the full signal. The correlation decays up to $k_2\eta \approx 0.3$, beyond which it remains constant. The constant value is significantly larger than that for the full-signal correlations. This feature again highlights that correlations between slow fluctuations are stronger for slow signals, particularly in the transfer. Wavenumbers in the BR are almost perfectly correlated in slow modes.

A similar analysis for fluctuations in E confirms that fluctuations are highly correlated across all wavenumbers with no significant R_λ trends. We have therefore not shown those data here.

Returning to figure 4, especially figure 4(*d*) for slow fluctuations, we saw that changes in E and T at large scales are highly correlated with changes at smaller scales, up to the NDR, with a time lag. This time lag increases with the distance between the scales being considered. As noted earlier, this is qualitatively consistent with classical cascade concepts. Note that the slope of the white markers in figure 4(*c*,*d*) can be

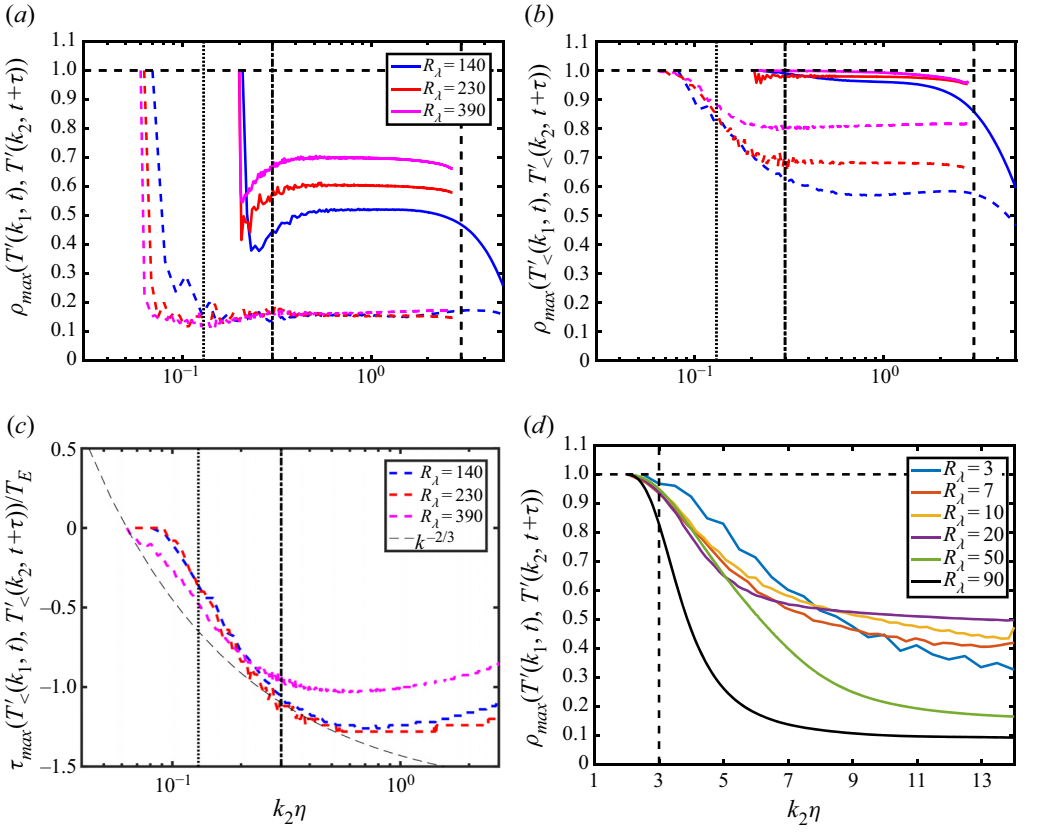

FIGURE 5. The maximum correlation coefficient (ρ_{max}) between (*a*) full and (*b*) slow modes of energy transfer functions. Dashed lines correspond to $k_1\eta \approx 0.06$ and solid lines to $k_1\eta \approx 0.2$. (*c*) Time lag corresponding to ρ_{max} in (*b*). (*d*) Maximum correlation coefficient ρ_{max} for $k_1\eta \approx 2$. Vertical lines are the same as in figure 2.

interpreted as the 'speed' of the transfer across scales. This information can be used to further our comparison to the classical cascade more quantitatively. The time scale associated with a scale $1/k$ can be estimated by knowing that its energy content is $E(k)k$. Dimensional analysis would then yield $T_c \propto 1/\sqrt{E(k)k^3}$, where T_c is the local time scale associated with $1/k$. In classical phenomenology, this is also the time associated with the transfer of energy to neighbouring smaller scales. In the IR, if $E(k) = C_k\langle\epsilon\rangle^{2/3}k^{-5/3}$, we obtain $T_c \approx C_k^{-1/2}\langle\epsilon\rangle^{-1/3}k^{-2/3}$, where $C_k \approx 1.6$–1.7 (Sreenivasan 1995; Donzis & Sreenivasan 2010). Finally, the total time taken by a perturbation in k_1 to reach k_2 would be the sum of all time intervals to cross the wavenumber interval. If wavenumbers are binned in octaves, for example, the total time is a sum of T_c across different bins (Tennekes & Lumley 1972; Lumley 1992). If one considers a continuum spectrum instead, one obtains

$$\tau_{k1\to k_2} = \int_{k_1}^{k_2} |\,\mathrm{d}T_c/\mathrm{d}k|\,\mathrm{d}k = C_k^{-1/2}\langle\epsilon\rangle^{-1/3}k_1^{-2/3}\left(1-(k_1/k_2)^{2/3}\right). \tag{4.1}$$

This can be normalized by the local cascade time scale $T_c(k_1) \approx C_1 T_E$, where C_1 is a proportionality constant of order unity relating T_E and T_c when k_1 is near the large scales.

Then

$$\frac{\tau_{k_1 \to k_2}}{T_E} = C_1 \left(1 - (k_1/k_2)^{2/3}\right). \tag{4.2}$$

This expression (also derived by Bos, Shao & Bertoglio (2007)) is compared against τ_{max} in figure 5(*c*), where the transfer fluctuations peak at later times with increase in k_2 within the IR. The measured lag times agree reasonably well with the expression (4.2) for $C_1 = 1.7$, shown as a dashed black line. Such a behaviour is in contrast to the full signal for which there is no readily identifiable time lag, as discussed earlier. This observation further supports the conclusion that the classical cascade occurs only for the slow signals. As noted earlier, for $k_2\eta > 0.3$ – that is, beyond the BR – in the energy transfer spectrum, we have a different behaviour in which the peak correlation is independent of wavenumber. These results are consistent with the results reported in Cardesa *et al.* (2015) and Meneveau & Lund (1994) where the authors studied the correlation between the subgrid-scale stress tensor for velocity fields filtered at different spatial subgrid scales.

The peak correlations for the FDR with a wavenumber in the NDR, shown in figure 5(*d*), lose the correlation rapidly in both energy and transfer fluctuations. The concept of cascade is not expected to be valid here as the scales are dominated by dissipation. These scales also show large fluctuations that oscillate rapidly. In addition, they are fully correlated with each other as confirmed in figure 1 by the constant correlation in figure 4 and figure 5(*d*) for $R_\lambda > 10$ and $k_2\eta \geq 6$. We note that the loss of correlation with increase in k_2 for all wavenumbers is only observed for $R_\lambda < 10$. This again emphasizes that the loss of correlation may be a low-R_λ feature. At higher R_λ, the correlation becomes approximately independent of k_2 in the FDR.

Finally, we comment on the relation between transfer and energy fluctuations at the same wavenumber. Because of the differential relation (3.1) between E and T, temporal changes in $T(k, t)$ will lead to temporal changes in $E(k, t)$ only after some delay. As a complement to the analysis above, one can look at the peak correlation between $T(k_1, t)$ and $E(k_1, t + \tau)$, now at the same wavenumber $k_1 = k_2 = k$. When k is the dissipative region, figure 6 shows that the peak occurs with zero delay but the delay increases in magnitude across the IR (marked by white dots). In other words, when the slow component of energy is transferred to a wavenumber in the IR, it takes longer and longer for that change to be observed in the energy at that same wavenumber. Over that period other energy exchanges to/from that wavenumber can take place, which may explain why signatures of a classical cascade are much clearer for T than for E. These to-and-fro exchanges may also explain why the oscillations around the average value are significantly damped out in the energy signals. Needless to say, no such behaviour is observed in the IR for the full signal.

5. Discussion and conclusions

When we force a flow at low wavenumbers, whether steadily or randomly, the resulting turbulent fluctuations develop significant temporal fluctuations. It is important to understand how these fluctuations are transmitted across wavenumber space. Here, we studied single-time and time-delay statistics of energy and energy transfer spectra using well-resolved isotropic direct numerical simulations for a range of Reynolds numbers, with two different forcing mechanisms (although results were presented for only the SF DIFdelforcing case). We found that the fluctuations in energy transfer in the IR and FDR are much larger than their time average. In the IR, the amplitude of the fluctuations at a given wavenumber decreases with increasing R_λ while in the FDR the fluctuations are in the form of (skewed) large intermittent bursts.

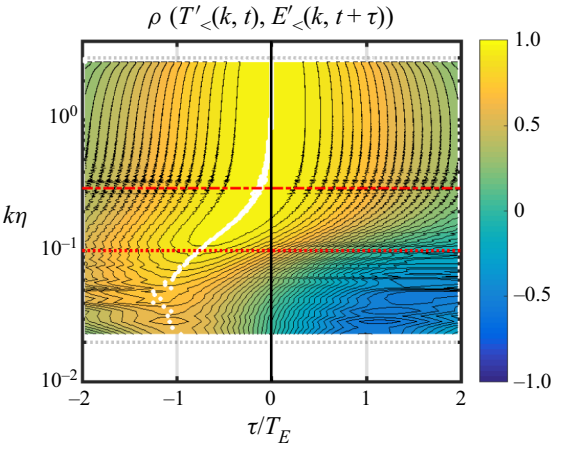

FIGURE 6. Contours of correlation at different time lags for slow modes of transfer and energy at the same scale ($k_1 = k_2 = k$) for $R_\lambda \approx 390$. Horizontal lines are the same as the vertical lines in figure 2. Solid black line is zero lag.

One main lesson is that the local cascade scenario is observed only for slow modes of energy transfer. Large-amplitude fast-time variations are present across the IR and tend to mask the inter-scale correlations observed for slow fluctuations. Rapid fluctuations cannot be transmitted through the large and inertial ranges, since the reaction time of these scales is too long. Indeed, there is some non-equilibrium basis for understanding the statistics of fast fluctuations in the IR (Yoshizawa 1994; Bos & Rubinstein 2017).

The second main lesson is that the energy transfer in the IR for the full signal is more like a slight imbalance between two opposing fluxes, oscillating up and down in time at any given k. We speculate that the fast modes, which are instantaneously felt across all wavenumbers, are signatures of significant non-local interactions in energy transfer at a given scale in the IR. The effect of the rapidly oscillating part is similar to decreasing R_λ, where a clear separation between largest and smallest scales is absent. Fluctuations in the FDR are uncorrelated with the IR and become increasingly so at high R_λ. For $R_\lambda > 10$, we found that the fluctuations at all wavenumbers in the FDR synchronize with each other (still uncorrelated from large scales). Similar synchronization was observed for fluctuations in both energy and energy transfer at wavenumbers $k\eta > 0.3$ which include the BR and NDR.

Acknowledgements

We thank Professor J. A. Domaradzki for his helpful comments on an earlier draft.

Declaration of interests

The authors report no conflict of interest.

REFERENCES

BATCHELOR, G. K. 1953 *The Theory of Homogeneous Turbulence*. Cambridge University Press.
BOS, W. J. T. & RUBINSTEIN, R. 2017 Dissipation in unsteady turbulence. *Phys. Rev. Fluids* **2**, 022601.

Bos, W. J. T., Shao, L. & Bertoglio, J. P. 2007 Spectral imbalance and the normalized dissipation rate of turbulence. *Phys. Fluids* **19**, 045101.

Brasseur, J. G. 1991 Comments on the Kolmogorov hypotheses of isotropy in the small scales. *AIAA Paper* (91-0230).

Brasseur, J. G. & Wei, C. H. 1994 Interscale dynamics and local isotropy in high Reynolds number turbulence within triadic interactions. *Phys. Fluids* **6**, 842.

Cardesa, J. I., Vela-Martín, A., Dong, S. & Jiménez, J. 2015 The temporal evolution of the energy flux across scales in homogeneous turbulence. *Phys. Fluids* **27**, 111702.

Domaradzki, J. A. 1988 Analysis of energy-transfer in direct numerical simulations of isotropic turbulence. *Phys. Fluids* **31**, 2747–2749.

Domaradzki, J. A. & Carati, D. 2007 An analysis of the energy transfer and the locality of nonlinear interactions in turbulence. *Phys. Fluids* **19**, 085112.

Domaradzki, J. A. & Rogallo, R. S. 1990 Local energy-transfer and nonlocal interactions in homogeneous, isotropic turbulence. *Phys. Fluids* **2**, 413–426.

Domaradzki, J. A., Teaca, B. & Carati, D. 2009 Locality properties of the energy flux in turbulence. *Phys. Fluids* **21**, 025106.

Donzis, D. A. & Sreenivasan, K. R. 2010 The bottleneck effect and the Kolmogorov constant in isotropic turbulence. *J. Fluid Mech.* **657**, 171–188.

Donzis, D. A. & Yeung, P. K. 2010 Resolution effects and scaling in numerical simulations of passive scalar mixing in turbulence. *Physica* D **239**, 1278–1287.

Eswaran, V. & Pope, S. B. 1988 An examination of forcing in direct numerical simulations of turbulence. *Comput. Fluids* **16**, 257–278.

Falkovich, G. 1994 Bottleneck phenomenon in developed turbulence. *Phys. Fluids* **6**, 1411–1414.

Frisch, U. 1995 *Turbulence*. Cambridge University Press.

George, W. K. & Wang, H. 2004 The spectral transfer in isotropic turbulence. In *IUTAM Symposium on Reynolds Number Scaling in Turbulent Flow* (ed. T. B. Gatskii, S. Sarkar & G. Speziale), pp. 223–228. Springer.

Horiuti, K. & Tamaki, T. 2013 Nonequilibrium energy spectrum in the subgrid-scale one-equation model in large-eddy simulation. *Phys. Fluids* **25**, 125104.

Ishihara, T., Morishita, K., Yokokawa, M., Uno, A. & Kaneda, Y. 2016 Energy spectrum in high-resolution direct numerical simulations of turbulence. *Phys. Rev. Fluids* **1**, 082403.

Kholmyansky, M. & Tsinober, A. 2008 Kolmogorov 4/5 law, nonlocality, and sweeping decorrelation hypothesis. *Phys. Fluids* **20**, 041704.

Khurshid, S., Donzis, D. A. & Sreenivasan, K. R. 2018 Energy spectrum in the dissipation range. *Phys. Rev. Fluids* **3**, 082601.

Kraichnan, R. H. 1977 Eulerian and Lagrangian renormalization in turbulence theory. *J. Fluid Mech.* **83**, 349–374.

Küchler, C., Bewley, G. & Bodenschatz, E. 2019 Experimental study of the bottleneck in fully developed turbulence. *J. Stat. Phys.* **175**, 617–639.

Lumley, J. L. 1992 Some comments on turbulence. *Phys. Fluids* A **4**, 203–211.

McComb, W. D. 2014 *Homogeneous, Isotropic Turbulence: Phenomenology, Renormalization and Statistical Closures*. Oxford University Press.

Meneveau, C. & Lund, T. S. 1994 On the lagrangian nature of the turbulence energy cascade. *Phys. Fluids* **6**, 2820–2825.

Mininni, P. D., Alexakis, A. & Pouquet, A. 2008 Nonlocal interactions in hydrodynamic turbulence at high Reynolds numbers: the slow emergence of scaling laws. *Phys. Rev.* E **77**, 036306.

Monin, A. S. & Yaglom, A. M. 1975 *Statistical Fluid Mechanics*, vol. 2. MIT Press.

Nelkin, M. & Tabor, M. 1990 Time correlations and random sweeping in isotropic turbulence. *Phys. Fluids* A **2**, 81–83.

Ohkitani, K. & Kida, S. 1992 Triad interactions in a forced turbulence. *Phys. Fluids* **4**, 794–802.

Praskovsky, A. A., Gledzer, E. B., Karyakin, M. Y. & Zhou, Y. 1993 The sweeping decorrelation hypothesis and energy–inertial scale interaction in high Reynolds number flows. *J. Fluid Mech.* **248**, 493–511.

Sagaut, P. & Cambon, C. 2018 *Homogeneous Turbulence Dynamics*. Springer.

SREENIVASAN, K. R. 1995 On the universality of the Kolmogorov constant. *Phys. Fluids* **7**, 2778–2784.

TENNEKES, H. & LUMLEY, J. L. 1972 *A First Course in Turbulence*. MIT Press.

VAN ATTA, C. W. & WYNGAARD, J. C. 1975 On higher-order spectra of turbulence. *J. Fluid Mech.* **72**, 673–694.

VERMA, M. K. & DONZIS, D. A. 2007 Energy transfer and bottleneck effect in turbulence. *J. Phys.* A **40**, 4401–4412.

YEUNG, P. K. & BRASSEUR, J. G. 1991 The response of isotropic turbulence to isotropic and anisotropic forcing at the large scales. *Phys. Fluids* **3**, 884–897.

YEUNG, P. K., SREENIVASAN, K. R. & POPE, S. B. 2018 Effects of finite spatial and temporal resolution in direct numerical simulations of incompressible isotropic turbulence. *Phys. Rev. Fluids* **3**, 064603.

YOSHIZAWA, A. 1994 Nonequilibrium effect of the turbulent-energy-production process on the inertial-range energy spectrum. *Phys. Rev.* E **49**, 4065.